

*2<sup>nd</sup> International School on Surface Science*



*"Technologies and Measurements on Atomic Scale"*

*1 – 7 October 2012, Khosta (Sochi), Russia*

## **Book of abstracts**

of the 2nd International School on Surface Science  
"Technologies and Measurements on Atomic Scale"



## **Preface**

The School's primary objective is to convey the state of the art in modern surface science and demonstrate theoretical and experimental ability to study single atoms or molecules adsorbed on solid state surfaces. First School was successfully held in Veliky Novgorod last year. Second School will also demonstrate multiple roles of a scanning probe microscope operating at cryogenic temperatures and in ultrahigh vacuum, the main experimental tool at the atomic scale. It can be used not only as an extremely high resolution microscope but also as a multipurpose spectrometer to study the electronic, vibrational and spin states of a designated object with atomic resolution.

All School's lecturers, both Russian and International, are leading figures in their respective parts of surface science. Lecture topics center around surface magnetism, model catalysis, surface phase transitions, quantum informatics, superconductive and strongly correlated systems, and low dimensional systems including carbon nanomaterials. The School is organized as a 7-day workshop in which lectures alternate with participants' own presentations.

## **Organizers**

Prokhorov General Physics Institute RAS and Sochi State University.

## **Program committee**

Prof. Konstantin N. Eltsov (Prokhorov General Physics Institute RAS, Moscow, Russia);

Prof. Alexander A. Saranin (Institute for Automation and Control Processes FEB RAS, Vladivostok, Russia);

Prof. Markus Morgenstern (Physikalisches Institut B and JARA-FIT, RWTH Aachen University, Germany).

## **Organizing committee**

Chairman: Prof. Konstantin N. Eltsov (Moscow);

Members: Prof. Nina M. Pestereva (Sochi), Dr. Lev M. Ghogarov (Sochi), Dr. Vladimir M. Shevlyuga (Moscow), Viktor V. Zheltov;

Secretary: Dr. Tatiana V. Pavlova (Moscow).

## **Sponsors**

Russian Academy of Science;

Russian Foundation for Basic Research;

Dynasty Foundation;

SPECS Surface Nano Analysis GmbH;

INTERTECH Corporation;

"RusMott" Co. Ltd.;

Systems for microscopy and analysis;

R&D company "Sigma Scan Ltd".

## Conference Program

### Students Oral Session

1

- 1 Substrate-mediated interactions between chlorine atoms adsorbed on Au(111) and Ag(111): Scanning Tunneling Microscopy and Density Functional Theory approach  
*V. Zheltov, B. Andryushechkin, G. Zhidomirov, K. Eltsov, B. Kierren*
- 2 Energy gap revealed by low-temperature scanning-tunneling spectroscopy of Si(111)-7x7 surface in illuminated slightly-doped crystals  
*A.B. Odobescu, S.V. Zaitsev-Zotov*
- 3 Spin-dependent avoided-crossing effect on quantum-well states in Al/W(110)  
*A.G. Rybkin, A.M. Shikin, D. Marchenko, A. Varykhalov, and O. Rader*
- 4 Photoemission-controlled tuning of pristine and doped graphene electronic structure  
*D. Usachov, A. Fedorov, O. Vilkov, V.K. Adamchuk, D.V. Vyalikh*
- 5 Realization of lateral p-n junction on (0001) Bi<sub>2</sub>Te<sub>3</sub> topological insulator  
*O.E. Tereshchenko, K.A. Kokh, S.V. Makarenko, V.A. Golyashov*
- 6 Electroluminescence of GaP<sub>x</sub>N<sub>y</sub>As<sub>1-x-y</sub> nanoheterostructures through a transparent electrode made of CVD graphene  
*A.V. Babichev, V.Y. Butko, M.S. Sobolev, E.V. Nikitina, N.V. Kryzhanovskaya, and A.Yu. Egorov*

### Students Poster Session

7

- 7 AFM and EBSD applied to study the nanostructure of the metals and of the alloys subjected to thermal stress  
*P.G. Ulyanov*
- 8 Hybrid polymer nanosystems based on ZnSe nanoparticles: AFM and XPS Study  
*K.I. Borygina*
- 9 Features of electronic and spin structure of graphene after Au and Bi intercalation  
*Anna A. Popova, A.G. Rybkin, A.M. Shikin, D. Marchenko, A. Varykhalov, and O. Rader*
- 10 Precision measurements of temperature Si-substrates in ultrahigh vacuum  
*V.E. Fahriev, R.Z. Bakhtizin*
- 11 Electronic energy structure of TiNi and TiNi-Cu alloys  
*B.V. Senkovskiy*
- 12 Low-temperature scanning tunneling microscopy and subsurface defects of Bi<sub>2</sub>Se<sub>3</sub>  
*A. Dmitriev, N. Fedotov, V. Nasretdinova, S. Zaitsev-Zotov*
- 13 Statistical analysis of AFM topography images of nanoparticles on flat surface  
*V. Sevriuk, I.V. Shalnev, P.N. Brunkov, A.A. Gutkin*
- 14 MBE growth of III-V-N materials on Si substrates  
*Maxim Sobolev*
- 15 Resistivity and thermopower of monolayered graphene  
*A.V. Babichev, V.E. Gasumyants, and V.Y. Butko*
- 16 Photoluminescence of graphene nanoribbon and nanotube composites  
*P.V. Fedotov, A.I. Chernov, A.V. Talyzin, A.G. Nasibulin, E.D. Obraztsova*
- 17 Raman diagnostics of onion-like carbon  
*A.V. Pershina, S.N. Bokova-Sirosh, E.D. Obraztsova, K.V. Elumeeva, A.V. Ishchenko, S.I. Moseenkov, V.L. Kuznetsov*
- 18 Optical spectroscopy of polymer systems containing single-wall carbon nanotubes  
*S.N. Bokova-Sirosh, E.D. Obraztsova, T.S. Mamonova, M.V. Shablygin, and Y.I. Yuzyuk*

- 19 Synthesis and characterization of  $\text{Bi}_2\text{Se}_3$  and  $\text{Bi}_2\text{Te}_3$  crystals and flakes  
*E.A. Obraztsova, N.A. Polgun, A.S. Orekhov, P.V. Shapkin, E.D. Obraztsova*
- 20 Ferromagnetic decoration of encapsulated single-walled carbon nanotubes  
*A.I. Chernov, E.D. Obraztsova, H. Kuzmany*
- 21 All-optical injection and control of photocurrents in unbiased graphene  
*Petr A. Obraztsov, Tommi Kaplas, Sergey V. Garnov, Yuri P. Svirko*
- 22 STM/STS study of steps at the surface of ternary compound  $\text{Bi}_2\text{Te}_2\text{Se}$   
*A.A. Kapustin, V.S. Stolyarov, and S.I. Bozhko*
- 23 XPS characterization of the surface of coarse-grained and nanostructured titanium and nitinol  
*D.M. Korotin, S. Bartkowski, E.Z. Kurmaev, M. Neumann, D.V. Gunderov, R.Z. Valiev*
- 24 Structure of adsorbed fibrinogen studied by single-molecule atomic force microscopy and molecular dynamics simulation  
*A.D. Protopopova, A.P. Tolstova, E.G. Zavyalova, A.M. Kopylov, V.A. Tverdislov, I.V. Yaminsky*
- 25 Influence of irregular growth of monoatomic steps during Si/Si(001) epitaxy on generation of surface defects  
*L.V. Arapkina, V.A. Chapnin, K.V. Chizh, L.A. Krylova, V.A. Yuryev*

**Index of Authors****27**

# Substrate-mediated interactions between chlorine atoms adsorbed on Au(111) and Ag(111): Scanning Tunneling Microscopy and Density Functional Theory approach

V.V. Zheltov<sup>1\*</sup>

B.V. Andryushechkin<sup>1</sup>, G.M. Zhidomirov<sup>1</sup>, B. Kierren<sup>2</sup>, K.N. Eltsov<sup>1</sup>

<sup>1</sup>A. M. Prokhorov General Physics Institute of Russian Academy of Sciences, 38 Vavilov Street, 119991 Moscow, Russia

<sup>2</sup>Institut Jean Lamour - UMR CNRS 7198 - équipe 102, Université H. Poincaré, Nancy, France

\*E-mail: [zheltov@kapella.gpi.ru](mailto:zheltov@kapella.gpi.ru), Phone: +7 905 532 18 13

## Abstract

In this work, we present a combined low temperature scanning tunneling microscopy (STM) and Density Functional Theory (DFT) study of the chlorine adsorption on Au(111) and Ag(111) at low coverages.

According to our STM measurements, chlorine forms chain-like structures on Au(111) and Ag(111) at submonolayer coverages ( $\theta < 0.1$  ML). In the contrast to the case of the  $(\sqrt{3} \times \sqrt{3})R30^\circ$  structure (0.33 ML) characterized by the Cl-Cl distance of 5.0 Å, we detected abnormally short distances of 3.8 Å within the chains for Au(111) and 4.5 Å for Ag(111) at low coverages.

To find out the driving forces of this unusual coupling of chlorine atoms, we performed the DFT calculations using the Vienna ab-initio simulation package (VASP). Indeed, the local minimum for two chlorine atoms on Au(111) corresponds to the geometry shown in Fig.1. We see that one Cl atom occupies fcc position, while the other one appears to be in the bridge position. The formation of the chains has been also tested with DFT. The third chlorine atom was placed in the 14 different positions around the pair of chlorine atoms, as shown in Fig.1. According to our calculations, the formation of the compact islands (positions 6,7,13,14) is strongly unfavorable, whereas making the chain (positions 1,2,9,10) is the most energetically favorable scenario for a third atom (at distances of 5.0 Å or 3.8 Å).

In the course of the optimization of atomic coordinates, we detected a significant perturbation of the upper gold layer. The calculations with frozen positions of the atoms in the gold substrate did not reproduce local minimum at 3.8 Å and the preferable quasi-one dimensional geometry of chlorine chains. In this connection, we believe the interaction between chlorine atoms on Au(111) to be mediated by the elastic substrate distortion.

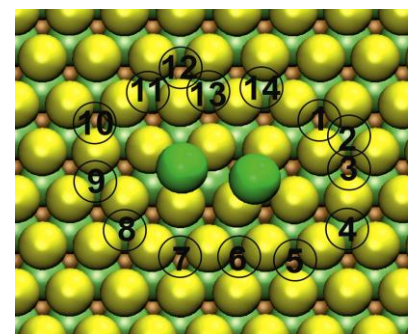


Fig. 1 Optimized structure model for two chlorine atoms on Au(111). Test positions for the third atom are indicated.

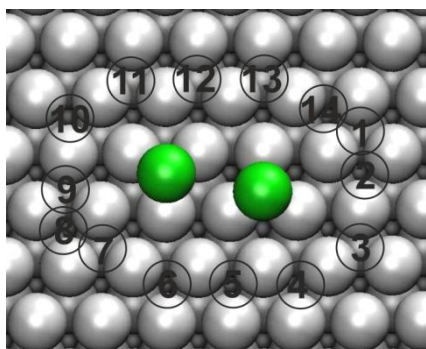


Fig. 2 Optimized structure model for two chlorine atoms on Ag(111). Test positions for the third atom are indicated.

In the case of Cl\Ag(111) the local minimum for two chlorine atoms corresponds to the geometry shown in Fig.2. We see that one Cl atom occupies fcc position, while the other one appears to be in the hcp position. The formation of the chains has been also tested with DFT by analogy with the gold substrate (Fig.2). According to our calculations, the formation of the compact islands (positions 5,6,12,13) is strongly unfavorable, whereas making the chain (positions 2,9) is the most energetically favorable scenario for a third atom (at distances of 5.0 Å or 4.5 Å). The calculations with frozen positions of the atoms in the silver substrate show that indirect electronic interaction plays significant role in formation of chlorine chain-like structures with short distances.

Thus, our calculations show that on Au(111) indirect elastic interaction between chlorine atoms predominates, on Ag(111) indirect electronic interaction between chlorine atoms predominates and this substrate-mediated interactions are strong enough to affect

the arrangement of chlorine atoms in the chain-like structures.

## Energy gap revealed by low-temperature scanning-tunneling spectroscopy of Si(111)-7x7 surface in illuminated slightly-doped crystals

A.B. Odobescu, S.V. Zaitsev-Zotov

Kotel'nikov IRE RAS, Mokhovaya 11, bld.7, 125009 Moscow, Russia

Physical properties of Si(111)-7x7 surface of low-doped Si samples are studied in a temperature range at 5 - 78K by the scanning-tunneling spectroscopy (STS). External illumination is applied to produce bulk conductivity required for STS measurements. Application of illumination removes completely the band bending near the surface and restores initial population of the surface states. Our results indicate the energy gap at surface Fermi level  $2\Delta = 40\pm 10$  meV in intrinsically populated Si(111)-7x7 surface. The gap vanishes at 35K.

Si(111)-7x7 is one of the most extensively studied crystal surface of semiconductors. It has a relatively high surface density of states with the Fermi level sitting inside of one of the surface zones, that leads to the metallic character of Si(111)-7x7 structure and experimentally has been confirmed at room temperature [1]. However, some experimental studies have demonstrated contradictory behavior. The dielectric gap with the value 70 meV [2] have been observed by STS for Si(111)-7x7 surface at 5K and below, also non-metallic behavior was found in the transport measurements [3]. The origin of such a discrepancy requires detailed study and understanding.

The STS studies of Si(111)-7x7 surface are usually carried out with using heavy-doped Si (typical resistivity  $\rho \sim 0.01 \div 0.001 \Omega\text{cm}$ ), especially at low temperatures measurements. Such a high doping level is necessary to provide a reasonable bulk conduction. But the effect of doping on the surface current carriers concentration is not negligible. A typical variation of the surface current carriers concentration is of the order of its value in heavy-doped crystals (for example the relative surface current carrier concentration change for samples with  $\rho \sim 0.001 \Omega\text{cm}$  can be estimated about 40%). Thus, in principle the effect of doping may be responsible for variation of physical properties of Si(111)-7x7 surface and need special consideration. In this case, study of low doped Si samples is preferable.

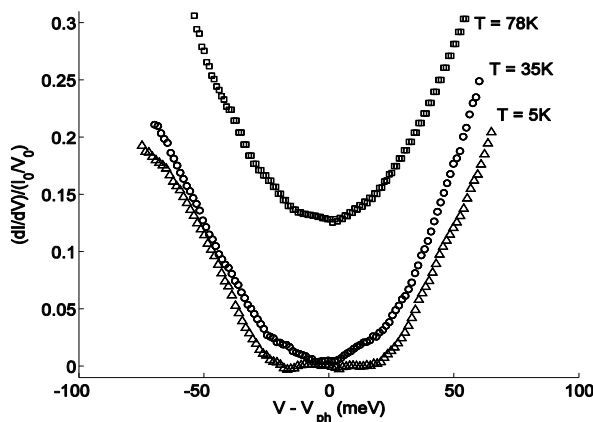


**Figure 1.** Normalized  $dI/dV$  curves of illuminated n-type,  $\rho = 1 \Omega\text{cm}$  Si(111)-7x7 surface in the gap region at different temperatures ( $\Delta$  - energy gap  $2\Delta = 40\pm 10$  meV at  $T = 5\text{K}$ ,  $\circ$  - energy gap vanishes at  $T = 35\text{K}$ ,  $\square$  - no gap at  $T = 78\text{K}$ ). Set points are  $V_0 = 2 \text{ V}$  and  $I_0 = 100 \text{ pA}$ ,  $V_{\text{ph}}$  - surface photovoltage originated from external illumination.

Here we report the results of our STS study of energy spectrum of Si(111)-7x7 surface in slightly doped n- and p-type Si with  $\rho \sim 1 \Omega\text{cm}$  in the range of 5 - 78 K under illumination, which was used to provide bulk conduction for STM measurements at this temperatures. The results confirm the existence of the dielectric energy gap at the surface Fermi level  $2\Delta = 40\pm 10$  meV at  $T = 5\text{K}$  on p-type and n-type crystals. With increasing the temperature the energy gap vanishes at 35K and completely disappears at higher temperatures (Fig.1), thus the Fermi level sits inside the surface band providing thereby the metallic conduction of the surface, in agreement with the general results [1].

Note, that the energy gap value of Si(111)-7x7 surface is the same in slightly doped p- and n-type samples, but is almost 2 times smaller than the gap value reported in Ref. [2] for heavily-doped samples.

Possible scenarios of gap opening include Mott-Hubbard mechanism assisted by electron-phonon interaction, formation of two-dimensional Wigner crystal or density waves. In most scenarios the smaller gap value corresponds to a bigger bare electron density of states of Si(111)-7x7 surface at the Fermi level.

[1] K. Oura, V.G. Lifshits, A.A. Saranin, A.V. Zotov, M. Katayama 2003 *Surface Science: An Introduction* Springer-Verlag, Berlin

[2] S. Modesti, H. Gutzmann, J. Wiebe, and R. Wiesendanger 2009 *Phys. Rev. B* **80** 125326

[3] T. Tanikawa, K. Yoo, I. Matsuda, S. Hasegawa, and Y. Hasegawa 2003 *Phys. Rev. B* **68** 113303

[4] J. Ortega, F. Flores, and A.L. Yeyati 1998 *Phys. Rev. B* **58** 4584

**Spin-dependent avoided-crossing effect on quantum-well states in Al/W(110)**A.G. Rybkin<sup>1</sup>, A.M. Shikin<sup>1</sup>, D. Marchenko<sup>1,2</sup>, A. Varykhalov<sup>2</sup>, and O. Rader<sup>2</sup><sup>1</sup>Physical department, St. Petersburg State University, St. Petersburg, 198504 Russia<sup>2</sup>Helmholtz-Zentrum Berlin für Materialien und Energie,  
Elektronenspeicherring BESSY II, Albert-Einstein-Str. 15, D-12489 Berlin, Germany

The unique features of the valence band electronic structure characteristic for different type low-dimensional systems and quantum objects determine in significant degree their unique electronic and physicochemical properties. However, these features can be significantly modified by interaction with electron states of the substrates where these systems are formed, for instance, due to the avoided-crossing effect. Due to this effect the corresponding hybrid states are formed under interaction between the states of the deposited metal (quantum-well states for low-dimensional systems) and the substrate which are located in the region of the assumed intersection between the interacting substrate and deposited metal states. It leads to the significant resulting modification of the observed dispersion dependences and appearance of kinks or gaps on these dispersions. On the other hand, the influence of substrate can also lead to a modification of the spin structure of the formed quantum systems and deposited metal overlayers. It was shown in refs. 1-3 that the deposition of thin films or monolayers of noble metals on W(110) is followed by pronounced spin-orbit splitting of quantum-well and interface states induced by the substrate. In these systems, a significant modification of the dispersion dependences was also observed in the region of the assumed intersection of quantum-well and substrate states.

The present work is devoted, on the one hand, to the analysis of the modification of the dispersion dependences of quantum-well and interface states formed in thin layers of light metal Al with different thickness on W(110) caused by their interaction with the substrate. On the other hand, it aims in clarification of the question how does the spin structure of the states can be modified under the „substrate-overlayer” interaction and how it can be explained from the positions of the spin-dependent avoided-crossing effect.

[1] A. M. Shikin, A. Varykhalov, G. V. Prudnikova, D. Usachov, V. K. Adamchuk, Y. Yamada, J. D. Riley, and O. Rader, *Phys. Rev. Lett.* 100, 057601 (2008).

[2] A. Varykhalov, J. Sánchez-Barriga, A. M. Shikin, W. Gudat, W. Eberhardt, and O. Rader, *Phys. Rev. Lett.* 101, 256601 (2008).

[3] A. M. Shikin, A. G. Rybkin, D. E. Marchenko, D. U. Usachov, V. K. Adamchuk, A. Varykhalov, and O. Rader, *Phys. Solid State* 52, 1515 (2010).

## Photoemission-controlled tuning of pristine and doped graphene electronic structure

D. Usachov<sup>1</sup>, A. Fedorov<sup>1</sup>, O. Vilkov<sup>1,2</sup>, V.K. Adamchuk<sup>1</sup>, D.V. Vyalikh<sup>1,2</sup>

<sup>1</sup> Faculty of Physics, St. Petersburg State University, 198504, St. Petersburg, Russia

<sup>2</sup> Institute of Solid State Physics, Dresden University of Technology, D-01062 Dresden, Germany

Graphene is a perspective material for future nanoelectronic devices. For variety of applications it is important to have possibility for selecting the required charge carriers type and controlling their concentration. Therefore, a variety of approaches for manipulating the graphene electronic and crystal structure attracts particular attention [1]. One of the most promising approaches for tuning the electronic properties of graphene is doping with heteroatoms, particularly with nitrogen or boron. Substitution of carbon atoms with nitrogen must lead to appearance of additional charge in the graphene conduction band, providing n-type conductivity [2]. On the contrary, boron is expected to form an acceptor-type impurity, making graphene a p-type semiconductor. The charge carriers concentration may be varied by controlling the concentration of dopant during the synthesis.

Here we discuss an efficient approach for tuning the graphene electronic structure by nitrogen and boron doping, studied with photoemission. It is shown that N- and B-doped graphene with notable concentration of impurities can be synthesized on nickel surface using CVD method. Foreign atoms, incorporated into graphene, usually have different types of bonding configurations. Each of them affects the electronic properties differently. Using the angle-resolved and X-ray photoemission spectroscopy we have analyzed the bonding configurations of impurities and estimated the doping efficiency by monitoring the Dirac cone position dependence on the type and concentration of impurities. Furthermore, in case of N-doped graphene it has been demonstrated that introduction of Au atoms to the graphene-Ni interface allows to achieve significant enhancement of the charge transfer due to the temperature-induced transition of N atoms to substitutional bonding configuration [3]. This also provides a possibility for fine tuning of the doping level in graphene.

The other important issue is the role of graphene interaction with the substrate, which may affect the graphene electronic structure in different ways. Here we discuss this phenomenon with recent examples of novel graphene-based systems.

This work was supported by the Ministry of Education and Science within the grant of the President of Russian Federation MK-3303.2012.2, and by RFBR and SPbSU grants.

[1] J.C. Meyer et al., *Nature Mater.* 10, 209 (2011)

[2] A. Lherbier et al., *Phys. Rev. Lett.*, 101, 036808 (2008)

[3] D. Usachov et al., *Nano Lett.* 11, 5401 (2011)

## Realization of lateral p-n junction on (0001)Bi<sub>2</sub>Te<sub>3</sub> topological insulator

O.E. Tereshchenko<sup>1,2</sup>, K.A. Kokh<sup>3</sup>, S.V. Makarenko<sup>1</sup>, V.A. Golyashov<sup>2</sup>

<sup>1</sup>*Institute of Semiconductor Physics SB RAS, 13, Lavrentieva prosp., Novosibirsk 630090, Russia*

<sup>2</sup>*Novosibirsk State University, 2, Pirogova str., Novosibirsk 630090, Russia*

<sup>3</sup>*Institute of geology and mineralogy SB RAS, 3, Koptyuga ave., Novosibirsk 630090, Russia*  
e-mail: teresh@isp.nsc.ru

Topological insulator (TI) is a strong spin-orbit coupling system, which makes possible to control the spin transport electrically. Three dimensional TIs represent a class of materials with specific spin-split surface states which provides unobstructed motion of electrons in the surface layer. Recently, theoretical proposal for fabricating the topological p-n junction has been made based on (Bi<sub>1-x</sub>Sb<sub>x</sub>)<sub>2</sub>Te<sub>3</sub> in which carrier type and density in two adjacent region are controlled by composition graded or electrical gating [1]. Such a device was not realized experimentally.

This report is focused on the preparation of single Bi<sub>2</sub>Te<sub>3</sub> crystal with as grown built in p-n junction formed perpendicular to the cleavage plane. Phase diagrams and growth conditions are discussed. As-received crystals, grown by modified Bridgman method using rotating heat field, were cleaved and characterized by Hall measurements, atomic force microscopy, scanning tunneling microscopy, and photoemission spectroscopy. Photoemission with spatial resolution was used to identify surface states in p- and n-type region.

It is known that Bi<sub>2</sub>Te<sub>3</sub> crystals can be grown both p- and n-type conductivity depending on the Bi/Te ratio in the solution. The transition from p- to n- type takes place when Te concentration in the solution is close to 61% and determined by the intrinsic defects. We assumed to receive switching from p- to n type using the effect of Te segregation in vertical Bridgman method and successfully realized built in p-n junction along the boule of Bi<sub>2</sub>Te<sub>3</sub>. The results demonstrate high crystallographic quality and chemical stability of the cleaved surfaces even after month of air exposure. In the vicinity of the p-n junction, Hall coefficient changed sign abruptly, electron concentration decreased by two orders of magnitude (down to 10<sup>17</sup> cm<sup>-3</sup>) and the electron mobility reached the value of 50000 cm<sup>2</sup>/Vs at 4 K. It was found that on both part of the (0001) surface (p- and n-type) 2D electron gas was formed caused by downward band bending. Possible effects of intermixing between topological surface state and 2D electron gas are discussed. The perspective of (Bi<sub>1-x</sub>Se<sub>x</sub>)<sub>2</sub>Te<sub>3</sub> using in TI p-n junction and spin-polarized states in this system will be considered.

[1] J. Wang, X. Chen, B.-F. Zhu, and S.-C. Zhang, Phys. Rev. B 85, 235131 (2012).

## Electroluminescence of GaP<sub>x</sub>N<sub>y</sub>As<sub>1-x-y</sub> Nanoheterostructures through a Transparent Electrode Made of CVD Graphene

**Babichev A.V.<sup>1,2</sup>, Butko V.Y.<sup>1,2</sup>, Sobolev M. S.<sup>1</sup>, Nikitina E. V.<sup>1</sup>, Kryzhanovskaya N. V.<sup>1,2</sup>, and Egorov A. Yu.<sup>1,2</sup>**

<sup>1</sup> *St. Petersburg Academic University, Nanotechnology Research and Education Centre, RAS,  
Khlopin street 8/3, St Petersburg, 195220, Russia*

<sup>2</sup> *Ioffe Physical Technical Institute, Russian Academy of Science (RAS),  
26 Polytechnicheskaya street, St Petersburg 194021, Russia*

We present results on fabrication and electroluminescence studies of GaP<sub>x</sub>N<sub>y</sub>As<sub>1-x-y</sub> nanoheterostructures with a new type of transparent graphene based electrode. The observed properties of these structures and their possible applications are discussed.

Transparent electrodes provide uniform current spreading over the semiconductor surface to obtain light emission from the entire surface of the semiconductor nanoheterostructure. Transparent electrodes made of indium tin oxide (ITO) are prone to degradation because of electrically stimulated migration and thermal and chemical instability. In comparison to ITO, graphene exhibits a number of advantages in addition to the higher transparency. Among these advantages are flexibility, chemical stability, and lower cost. Chemical vapor deposition (CVD) of graphene is one of the most promising methods for the production of graphene for practical optoelectronic applications. The advantages of this technology are the high rate of graphene production, the feasibility of fabricating large-area samples, and its low cost. Due to recent progress it has become possible to form graphene sheets that are rather large in area and to transfer them directly onto the surface of semiconductor heterostructures for optoelectronic device fabrication.

The new class of GaP<sub>x</sub>N<sub>y</sub>As<sub>1-x-y</sub> alloys has huge potential in the production of optoelectronic devices capable of being integrated into silicon-based electronics. First, GaP<sub>x</sub>N<sub>y</sub>As<sub>1-x-y</sub> alloys can be grown on Si substrates pseudomorphously, with retention of the high structural quality. Second, the addition of even a relatively small amount of nitrogen results in formation of a direct band gap structure and opens up possibilities for producing efficient optoelectronic devices, including those based on silicon [1, 2]. Compared to commercial LEDs based on AlInGaP quantum wells, LEDs based on GaP<sub>x</sub>N<sub>y</sub>As<sub>1-x-y</sub> are expected to demonstrate improved wavelength stability of the emission in a broad range of injection currents and temperatures. Thus, LED nanoheterostructures based on GaP<sub>x</sub>N<sub>y</sub>As<sub>1-x-y</sub> alloys with a new type of CVD graphene transparent electrode offer promise for industrial applications.

We have studied *p-i-n* diodes with GaP<sub>x</sub>N<sub>y</sub>As<sub>1-x-y</sub> QWs separated by GaP barrier layers. The conductive CVD-graphene electrode was formed on the surface of the nanoheterostructures. The conditions for synthesis

of the CVD graphene layers were similar to those described elsewhere [3]. The subsequent transfer of CVD graphene onto the semiconductor surface has been done via procedure described in [4] with some modifications.

The CVD graphene electrode provides a substantial increase of the charge carrier spread from the edge of the metal electrodes.

The electroluminescence spectra have been recorded from the GaPNAs/GaP LED structures through a transparent graphene electrode in the temperature range from 12 to 60°C and the injection current from 0 A to 1 A.

The observed properties of these structures and their possible applications will be discussed.

An intense EL signal is observed at wavelengths close to 650 nm. High stability of the emission wavelength (2–3 nm) has been demonstrated in the temperature range from 12 to 60°C and the injection current from 0 A to 1 A. These result to be compared to the commercial AlInGaP LEDs properties that exhibit a 13 nm shift of the EL peak (from 500 to 603 nm), as the pump current is increased from 10 to 60 mA [5].

We acknowledge support from the Presidium of the Russian Academy of Sciences (2012-2014 years), research programs; the RFBR project nos.09-02-01444-a and 10-02-00853-a; FP7 Collaborative European Project № 257511 EU-RU.NET.

1. W. Shan et al., *Appl. Phys. Lett.* **76**, 3251 (2000).
2. I. A. Buyanova et al., *Appl. Phys. Lett.* **52**, 81 (2002).
3. K. S. Kim, Y. Zhao, H. Jang, S. Y. Lee, J. M. Kim, K. S. Kim, J.-H. Ahn, P. Kim, J.Y. Choi, and B. H. Hong, *Nature* **457**, 706 (2009).
4. X. Li, Y. Zhu, W. Cai, M. Borysiak, B. Han, D. Chen, R. D. Piner, L. Colombo, and R. S. Ruoff, *Nano Lett.* **9**, 4359 (2009).
5. V. A. Odnoblyudov and C. W. Tu, *J. Vac. Sci. Technol. B* **24**, 2202 (2006).

## AFM and EBSD applied to study the nanostructure of the metals and of the alloys subjected to thermal stress

P.G. Ulyanov

*Saint-Petersburg State University, Ulianovskaya Str. 1, 198504 St.-Petersburg, Petershof, Russia*

Carbon steels play important role in different spheres of industry as widely used constructional materials. The detailed knowledge of their microstructure is required for estimation of their residual life. Detailed microstructure analysis is provided by optical metallography, which deals with the mechanically polished and chemically milled steel surface. However the resolution of the optical microscope is rather limited. The use of probe microscopy techniques allows deeper analysis of microstructure, allowing quantitative imaging on nanometer scale.

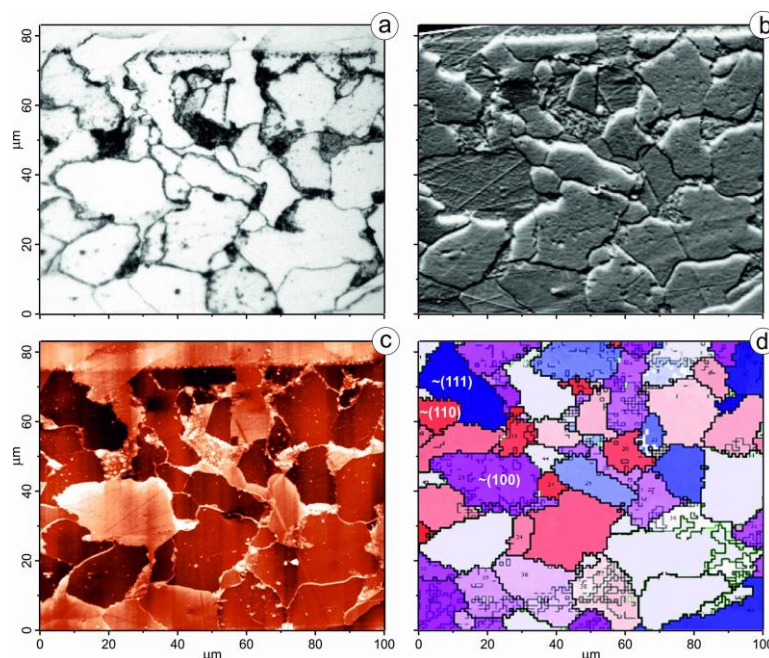


**Fig. 1.** Microscopy data, showing ferrite grains with different crystallographic orientations.

This work is aimed to study the mechanism of the surface relief formation upon chemical etching of the carbon steel surface with nital for subsequent microstructure analysis by means of AFM. Here we discuss the results of microscopic studies of this process by means of AFM, scanning electron microscopy (SEM) and electron backscatter diffraction (EBSD) (Fig. 1). The quantitative analysis of the etch rate dependence on the surface crystal structure of individual grains is presented and potential applications of scanning probe techniques for quantitative metallography are discussed.

This work was supported by the Ministry of education and science of the Russian Federation (Resolution 218).

## Hybrid Polymer Nanosystems Based on ZnSe nanoparticles: AFM and XPS Study

K.I. Borygina

*Saint-Petersburg State University, Ulianovskaya Str. 1, 198504 St.-Petersburg,  
Petershof, Russia*

The atomic force microscopy (AFM) is a powerful tool for studying physical and chemical properties of surfaces with subnanometre resolution. X-ray photoelectron spectroscopy (XPS) is a surface chemical analysis technique that can provide detailed information about complex biological systems. In this work a comprehensive AFM and XPS investigations of binary and ternary hybrid nanosystems based on zinc selenide (ZnSe) nanoparticles, stabilized by ampholitic biopolymer - bovine serum albumin (BSA), and polymethacrylic acid (PMAA) without and in the presence of a photosensitizer Photoditazin<sup>TM</sup> (PD) were performed. The objects of study were samples prepared from aqueous solutions of colloidal nanoparticles of ZnSe with polymer stabilizer, which were deposited on a silicon substrate. According to the XPS analysis of the core levels chemical shifts it was shown that the Zn and Se atoms form the ZnSe compound. XPS spectra of Zn 2p core level and Se 3p nanoparticles ZnSe, stabilized by polymers show that the chemical shifts  $\Delta\text{Zn } 2p$  and  $\Delta\text{Se } 3p$  are + 0.7 eV and - 0.7 eV, respectively. This means that the Zn and Se atoms are in a chemical compound ZnSe, in which the more electronegative selenium pulls over to the electronic density of zinc atoms.

By AFM it was shown that in the thin films of nanosystem ZnSe/BSA+PD on solid substrate forms the dense structures with the shape close to spherical. AFM images and the profile of the surface area, selected on the AFM images, show that the average nanostructure size is approximately 90 nm in diameter, and 6-8 nm in height. At the same time, the nanosystem ZnSe/PD+BSA consist of nanostructure approximately 150-200 nm in diameter, with the height of the clusters of the order of 1 nm. The results are oriented towards the development of new generation drugs for selective photodynamic therapy in oncology.

This work was performed within the framework of the Research Education Center "Nanostructures and Self Organization in Functional Macromolecular Systems and Their Diagnostics" and was supported by the RFBR, grant 10-03-01075.

The present work is the result of cooperation between the group of Prof. V.K. Adamchuk from the Saint-Petersburg State University, the laboratory of Prof. T.E. Sukhanova from the Institute of Macromolecular Compounds RAS and the group of Prof. M.L. Gelfond from the N. N. Petrov Federal Research Institute of Oncology of the Minzdravsocrazvityja.

## Features of electronic and spin structure of graphene after Au and Bi intercalation.

Anna A. Popova<sup>1</sup>, A.G. Rybkin<sup>1</sup>, A.M. Shikin<sup>1</sup>, D. Marchenko<sup>1,2</sup>, A. Varykhalov<sup>2</sup>, and O. Rader<sup>2</sup>

<sup>1</sup>Physical department, St. Petersburg State University, St. Petersburg, 198504 Russia

<sup>2</sup>Helmholtz-Zentrum Berlin für Materialien und Energie,  
Elektronenspeicherring BESSY II, Albert-Einstein-Str. 15, D-12489 Berlin, Germany

[popova.anna@bk.ru](mailto:popova.anna@bk.ru)

Graphene monolayer is a promising material of the nanoelectronics and spintronics due to its unique physicochemical properties and distinctive electronic energy and spin structure. Our recent investigations [1-4] showed that graphene synthesized on Ni(111) by cracking of propylene with subsequent intercalation of Au underneath the synthesized graphene monolayer is characterized by features of the electronic structure characteristic of quasi-free graphene and the possibility of an anomalously large spin-orbit splitting of  $\pi$ -states of graphene induced by the interaction with the underlying substrate. Experiments showed that the resulting value of the splitting can be changed from one to another experiment in the range from 10-15 meV and till 100 meV depending on the experimental conditions of the experiments and the ordering of the formed system. Interaction of graphene/Ni(111) with a substrate and followed intercalation of Cu underneath of graphene also doesn't reduce to a visible spin-orbit splitting of  $\pi$  states of graphene [1].

All these effects can be explained in the following way. First of all, Au is a heavy metal with a high atomic number ( $Z=79$ ) that testify for high value of gradient of intra-atomic potential at interface between graphene and underlying Au layer and which is cause of high value of surface-induced spin-orbit splitting of  $\pi$  states of graphene. Cu and Ni ( $Z=29$  and  $28$ ) is metals with a low atomic number, so intercalation of Cu or Ni atoms underneath graphene doesn't reduce to spin-orbit splitting of states of graphene. Secondly, in the presence of valence d states in substrate an increase of effects of spin-orbit splitting takes place, because of interaction of d states of metal with  $\pi$  states of graphene leads to hybridization of these states. We have shown that intercalation of the sp metal Bi, despite its high atomic number, does not lead to any noticeable spin-orbit splitting of  $\pi$  states of graphene. This means for a substrate-induced spin-orbit splitting in graphene  $\pi$ -states that the presence of d-states alone as in Cu and the high atomic number as in Bi are insufficient and their combination as in Au is required.

Investigations were carried out by the method of angle- and spin-resolved photoemission spectroscopy with application of synchrotron radiation at Helmholtz Center Berlin, BESSY II. Atomic and crystalline structure of the formed systems were analyzed by low energy electron diffraction and scanning tunneling microscopy.

### References:

1. A.M. Shikin, A.G. Rybkin, D. Marchenko, A.A. Popova, M.R. Scholz, O. Rader, A. Varykhalov "Induced spin-orbit splitting in graphene: role of atomic number of intercalated metal and  $\pi$ -d hybridization", submitted to New J. Phys.
2. A.Varykhalov, J. Sanchez-Barriga, A.M. Shikin, C. Biswas, E. Vescovo, A. Rybkine, D. Marchenko, O.Rader "Electronic and magnetic properties of quasi-free standing graphene on Ni", Phys. Rev. Lett. **101**, 157601 (2008).
3. D. Marchenko, A. Varykhalov, M.R. Scholz, E. Rashba, G. Bilmayer, A. Rybkin, A.M. Shikin, O. Rader „Giant Rashba splitting, band topology and hybridization at the graphene-Au interface“, submitted for publication.
4. D. Marchenko, A. Varykhalov, A. Rybkin, A.M. Shikin, O. Rader "Atmospheric stability and doping protection of noble-metal intercalated graphene on Ni(111)", Appl. Phys. Lett. **98**, 122111 (2011).

## Precision measurements of temperature Si-substrates in ultrahigh vacuum

V.E. Fahriev, R.Z. Bakhtizin.

Department of Physical Electronics and nanophysics, Bashkir State University, Ufa 450074,  
Russia.

## Abstract.

The quality and structure of the silicon surface reconstruction obtained during STM-investigations with atomic resolution is strongly dependent on the conditions of the Si-substrate prior to the study. Therefore when we try to receive the reconstructed surfaces of Si (111) at UHV conditions by one of important parameters is the temperature. The presented device allows quickly adjust the temperature of the sample by varying the current through the substrate, during measurements to obtain the necessary reconstruction of the surface of Si. The device is designed to improve the efficiency of experimental studies. Setting controls the process of preparation of the sample in an ultrahigh vacuum directly to STM - research. accurately determines the temperature of the Cu-substrate in UHV-installed with a pyrometer, integrated with a personal computer. Heating the Si-substrate is implemented in a standard way by passing a current through it. Samples were mounted on a tantalum sample holder using 'Ni-free' tools and the surface was cleaned by outgassing overnight at 650 °C [1]. The temperature is measured through the inspection hole of molybdenum glass in UHV chamber. Photodetector and the device are outside of vacuum chamber, making it a versatile and applicable in almost any standard ultra high vacuum system. Focal distance to the object can be set within 120-160 mm, while spot diameter of sight no more than 3 mm. The device allows researcher to control temperature, and watch for changes in temperature by adjusting the current through the sample, the performance of more than 1kHz. It is thus possible to produce more than 1000 measurements of temperature and current through adjustments per second, comply with these conditions the experimenter cannot afford in the performance of these procedures in a standard manual. The instrument is based on an optical pyrometer converter OPP-94, produced by Ufa Scientific and Technological Enterprise "Molnia". Standard measuring range is configured to measure the new values of the object temperature from 600 to 1300 °C. The structure of the device consists of the optical part and the electronic part. Electronic component, designed to interface with a PC for control, visualization and data storage. The optical part of a lens and a flexible optical fiber bundle, electronic part consists of a photodiode, which is joined with a flexible fiber bundle, feedback unit for current control and communication with a PC. An important feature is that it can be used to most accurately reproduce the conditions for a consistent series of STM - studies of the surface.

## References

- [1] T. Sakurai, T. Hashizume, et al., Prog. Surf. Sci. 33 (1990) 3.

**ELECTRONIC ENERGY STRUCTURE OF TiNi AND TiNi-Cu ALLOYS****B.V. Senkovskiy***Saint-Petersburg State University, Saint-Petersburg, Russia*

senkovskiy@gmail.com

type of presentation: poster

Electronic energy structure of the TiNi and TiNi-Cu alloys has been investigated both theoretically and experimentally. Experimental information about occupied and unoccupied density of states has been obtained by surface-sensitive techniques: X-ray photoelectron spectroscopy (XPS) and near edge X-ray absorption fine structure spectroscopy (NEXAFS). Particular attention was focused on *in situ* preparation of clean sample surfaces. Calculations were carried out using the full potential local orbital (FPLO) codes within generalized gradient approximation (GGA) for the exchange-correlation potential.

Theoretical model of the Ni and Ti electron redistribution in the TiNi and TiNi-Cu alloys relatively pure metals is found to be in a good agreement with experiments. It is found that the changes in Ti *d*-band occupancies in the TiNi alloy relative to the pure Ti take place due to intra-atomic electron redistribution between valence *d*- and *sp*-states. We have demonstrated that Ti *d*-state occupancy in the TiNi-Cu alloys is determined by chemical composition of the alloy and reaches a minimum in the TiNi alloy. It is assumed that with increasing Cu concentration in the TiNi-Cu alloys Ti *d*-electrons can form a direct covalent bonds, which reduce the temperature of martensitic transformation B19→B19' in Cu-rich TiNi-Cu alloys.

The author thanks his supervisor Prof. V.K. Adamchuk, A.G. Chikina for theoretical calculations, Dr. D.Yu. Usachov for helpful discussions, Dr. A.V. Shelyakov from National Research Nuclear University “MEPhI” (Moscow) for supplying the samples of alloys, O.Yu. Vilkov and A.V. Fedorov for experimental assistance at the Russian-German laboratory of the BESSY II synchrotron radiation center (Berlin).

This work was supported by RFBR 10-08-00580 and SPbSU grants.

## Low-temperature scanning tunneling microscopy and subsurface defects of $\text{Bi}_2\text{Se}_3$

A. Dmitriev, N. Fedotov, V. Nasretdinova, S. Zaitsev-Zotov  
Kotel'nikov IRE RAS, Mokhovaya 11-7, Moscow, 125009, Russia.

Topological insulators are a new class of materials with unique electronic properties. They are semiconductors in the bulk and have a metallic surface. Its conductivity is related to topologically protected Dirac-like electronic states. Spin and wave vector of an electron in such a state are correlated [1] so that an electron cannot scatter backwards without changing the direction of its spin, which is impossible in absence of a magnetic field.  $\text{Bi}_2\text{Se}_3$  is a well-known material of this class. Its crystalline structure consists of five-layer slabs Se-Bi-Se-Bi-Se.

Crystals of this compound were grown from a stoichiometric mixture of Se and Bi with 3% Se excess. As a result, p-type  $\text{Bi}_2\text{Se}_3$  samples were prepared, in contrast to usually studied n-type samples. The surface for STM study was prepared by cleavage under UHV conditions. Typical STM image of the sample surface is shown in fig.1. Three types of triangular defects of different size are discernible --- we call them t1, t2 and t3. We attribute these features to subsurface Bi defects in different atomic layers. Defects corresponding to bigger triangles lie deeper beneath the surface.

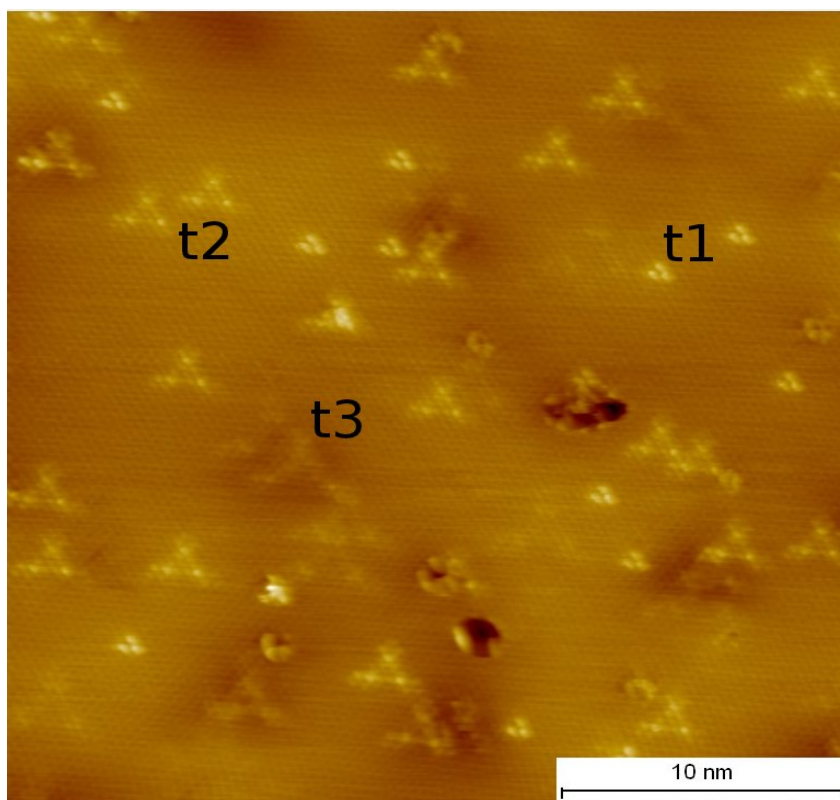


**Fig.1.**  $\text{Bi}_2\text{Se}_3$  surface with t1, t2 and t3 triangles.  $T=78\text{ K}$ ,  $V=-0.4\text{ V}$

1. M. Zahid Hasan, David Hsieh, Yuqi Xia, L. Andrew Wray, Su-Yang Xu, and Charles L. Kane, « A new experimental approach for the exploration of topological quantum phenomena», arXiv:1105.0396

## Statistical analysis of AFM topography images of nanoparticles on flat surface

V. Sevriuk\*, I.V. Shalnev\*\*, P.N. Brunkov\*\*, A.A. Gutkin\*\*

\* St Petersburg Academic University — Nanotechnology Research and Education Centre of the Russian Academy of Sciences

\*\* Ioffe Physical-Technical Institute of the Russian Academy of Sciences

At present the atomic force microscopy (AFM) is widely used to study nanoparticles. In the paper the special mathematical treatment is applied to AFM topography images of nanoparticles placed on flat surfaces to extract statistical parameters (size distribution, average distance between particles etc) of the nanoparticle arrays which contain a large number of pieces (more than a few hundred). The main problem of the treatment is due to the fact that in practice the flat surfaces are not really flat. Typically on distance of a few  $\mu\text{m}$  there is roughness of a few nm, which comparable with the size of nanoparticles. Because of that it is quite complicate to find automatically all nanoparticles on the AFM topography images. To solve the problem it is suggested a special AFM image processing based on the Laplacian of Gaussian (LoG) filter [1]. The optimal relations between size and shape of the LoG filter matrix and size of the AFM topography image matrix is discussed.

The statistical treatment was applied to study gold nanoparticles on mica surface, detonation nanodiamonds on the silicon surface and InAs self-organized quantum dots on GaAs surface.

1. Marr, D., Hildreth, E., 1980. Theory of edge detection. Proc. R. Soc. Lond. B Biol. Sci. 207, 187–217.

## MBE GROWTH OF III-V-N MATERIALS ON SI SUBSTRATES

III–V dilute nitride semiconductors such as  $\text{GaP}_{1-x}\text{N}_x$  currently attract extensive interest for their potential applications in microelectronic and optoelectronic devices. The incorporation of a small amount of nitrogen in a GaP matrix leads to a huge band gap bowing, and produces strong effects in the energy band structure resulting in a change from an indirect to a direct band gap material. Experimentally the band structure change was observed at very small nitrogen concentrations of  $x=0.005$ . In general,  $\text{GaP}_{1-x}\text{N}_x$  thin films have been grown employing technique of molecular beam epitaxy (MBE).

This class of dilute nitride material system has a tremendous application potential in silicon photonics, as the novel material system is shown to have a direct band structure and as it can be grown without the formation of extended defects on silicon substrates.

$\text{GaP}_x\text{N}_y\text{As}_{(1-x-y)}/\text{GaP}$  lattice-matched multiple quantum well (MQW) structures have been grown by MBE on GaP and Si substrates. Calculation of the  $\text{GaP}_x\text{N}_y\text{As}_{(1-x-y)}$  alloys band gap and approximated values of the hybridization parameter of the GaP conduction band and the localized nitrogen level are also presented in this work. Optical properties of  $\text{GaP}_x\text{N}_y\text{As}_{(1-x-y)}$  heterostructures grown on GaP(100) substrate have been studied by photoluminescence technique in 15-300K temperature range. The investigated heterostructures are quantum wells  $\text{GaP}_{0.814}\text{N}_{0.006}\text{As}_{0.18}$  (5 nm), separated by GaP barrier layers (5 nm), with different number of periods. Intense photoluminescence line has been observed in the spectral range 620-650 nm under optical excitation of the structures. The results of the investigations confirm the possibility to grow effective optoelectronic devices based on  $\text{GaP}_x\text{N}_y\text{As}_{(1-x-y)}$  alloys.

## Resistivity and thermopower of monolayered graphene

**Babichev A.V.**<sup>1,2</sup>, Gasumyants V.E.<sup>3</sup>, and V.Y. Butko\*<sup>1,2</sup>

<sup>1</sup> St. Petersburg Academic University, Nanotechnology Research and Education Centre, RAS,  
Khlopin street 8/3, St Petersburg, 195220, Russia

<sup>2</sup> Ioffe Physical Technical Institute, Russian Academy of Science (RAS),  
26 Polytechnicheskaya street, St Petersburg 194021, Russia

<sup>3</sup> St. Petersburg State Polytechnical University,  
29 Polytechnicheskaya street, St Petersburg 195251, Russia  
\*e-mail: vladimirbutko@gmail.com

We present results of our low temperature resistivity and thermopower coefficient measurements in graphene fabricated by Chemical Vapor Deposition technique.

Graphene are currently considered to be a material for post silicon technological era. There are two basic methods of graphene fabrication that can be useful for practical purposes. The first method is chemical vapour deposition (CVD) characterized by low cost, high rate of graphene production, and large sizes of the fabricated samples. The second method is thermal decomposition of SiC (ThD) while being compatible with silicon technology is quite expensive.

Among the most promising applications of graphene are RF transistor applications. In fact very high values of cutoff frequency  $f_t$  of transistors structures of 280 GHz [1] (ThD technique) and of 200 GHz [2] (CVD method) have been demonstrated. The features of transfer process of CVD graphene [3] can lead to additional scattering of charge carriers (mainly related to disorder at the interface), that affects RF characteristics of transistor structures.

Therefore transport properties of CVD graphene are very important object of investigation. The study of temperature dependence of resistivity ( $\rho$ ) and thermopower coefficient ( $S$ ) is effective tools for clarification of scattering mechanisms of charge carriers. However  $S(T)$  low experimental measurements were fulfilled only on graphene fabricated by ThD technique. (CVD-graphene thermopower coefficient measurements were performed only at room temperatures and above [4-6]).

We have studied  $\rho$  and  $S$  in a single layer of CVD-graphene samples up to 10mm×10 mm size, grown on copper foil. This technique allows to obtain monolayered graphene due to the low carbon solubility in copper. All our graphene samples was transferred on glass substrates with thickness of ~150  $\mu\text{m}$  to eliminate a possible contribution of a leakage current through the thin dielectric. Our samples were annealed during 4 hours in vacuum or in nitrogen at 573 K before the measurements.

The obtained room temperature resistivity values are in the range  $(1.7\div 4.1)\times 10^{-5}$  Ohm·cm. We have observed a constant resistivity from room temperature down to  $T=77.3$  K probably due to the weak dependence of the Fermi energy in this temperature range. Our measurements made in 4-layered graphene grown on nickel reveal weak  $\rho(T)$  with decreasing temperature. ( $\rho$  values typically increases by 7-9% with temperature decrease from 300 to 77 K). This difference can be explained under assumption that narrow band gap opens in graphene due to imperfection of the CVD grown samples.

The measured  $S(T)$  temperature dependence demonstrates a metallic behavior with hole type of conductivity. The peak related to phonon drag does not appear in the range of temperature  $T=77\div 300$  K. The values of  $S(T=300$  K) are about 40÷50  $\mu\text{B}/\text{K}$ . The thermopower coefficient in these samples decreases with temperature from 300 to 77 K. This thermopower coefficient drop in a single layer graphene is significantly larger compared to the drop in 4 layered graphene samples.

Our data are different from the data obtained by other [7]. This difference is probably indicates that graphene properties are strongly depend on the fabrication process.

We are grateful to Y.A. Kumzerov, A.Y. Egorov, and E. Nikitina for help. We acknowledge support from the Presidium of the Russian Academy of Sciences (2012-2014 years), research programs; the RFBR project 10-02-00853-a; and FP7 Collaborative European Project № 257511 EU-RU.NET.

1. Y. Q. Wu et al., Electron Devices Meeting (IEDM), 2011 IEEE International, 23.8.1 - 23.8.3 (2012).
2. P. Asbeck, K. Lee and J.-S. Moon, Wireless and Microwave Technology Conference (WAMICON), 2011 IEEE 12th Annual, 1-6 (2011).
3. Yu-Ming Lin et al., IEEE ELECTRON DEVICE LETTERS, **32** (10), 1343-1345 (2011).
4. A. N. Sidorov et al., Applied Physics Letters, **99**, 013115 (2011).
5. D. Sim et al., J. Phys. Chem. C, **115**, 1780-1785 (2011).
6. N. Xiao et al., ACS Nano, **5** (4), 2749-2755 (2011).
7. X.Wu et al., Applied Physics Letters, **99**, 133102 (2011).

## PHOTOLUMINESCENCE of GRAPHENE NANORIBBON and NANOTUBE COMPOSITES

P.V. Fedotov<sup>1</sup>, A.I. Chernov<sup>1</sup>, A.V. Talyzin<sup>2</sup>, A.G. Nasibulin<sup>3</sup>, E.D. Obraztsova<sup>1</sup>

<sup>1</sup> A.M. Prokhorov General Physics Institute, RAS, 38 Vavilov str., Moscow, Russia.

<sup>2</sup> Department of Physics, Umeå University, S-90187 Umeå, Sweden

<sup>3</sup> NanoMaterials Group, Aalto University, P.O. Box 15100, 00076 Aalto, Espoo, Finland  
fedotov@physics.msu.ru

SWCNTs are one of the most exciting materials today. They appeared to be extremely useable in various fields of applications. One of the most fascinating methods of utilizing nanotubes is to use them as a template for synthesis of other extraordinary nanomaterials or even as a supporting construction for unique (not existing in the suspended state) ones. The ultimate mechanical, chemical and physical properties of SWCNTs, basically, their stability upon various stress and a specific quasi-one-dimensional electronic structure and a tunability of their geometry, make them perfect candidates for the above-mentioned area of applications. The novel structures, properly designed in this way, as well as SWNT-based composites would possess unique properties and find a wide variety of applications.

An optical absorption spectroscopy, a photoluminescence spectroscopy and a Raman spectroscopy proved to be the efficient methods to characterize SWNTs. Moreover, in combination these analytical optical methods can be even more efficient, especially for description of SWNT-based composites.

In this work we tried to characterize SWNTs with graphene nanoribbons (GNR) inside using a combination of optical techniques. Such composites were synthesized using confined polymerization and fusion of polycyclic aromatic hydrocarbon (coronene) molecule by annealing in argon.

Raman measurements of these very composites prove presence of coronene based structures. Radial breathing mode of SWNTs in composites is shifted - over  $8\text{ cm}^{-1}$  - implying effective encapsulation. On the contrast, G-mode is not shifted - below  $0.5\text{ cm}^{-1}$ . The absorption bands of GNR@SWNT are red shifted and broadened. Photoluminescence (PL) map of the composites have extremely complicated original structure in UV-Vis range (Fig. 1). IR PL peaks of the nanotubes in composites experience systematic shift depending on the geometry.

*The work was supported by RAS research programs and MK-5618.2012.2*

[1] A.V. Talyzin et al., *NanoLetters* 11 (2011) 4352.

[2] Toshiya Okazaki, *Angew. Chem. Int. Ed.*, 50 (2011) 4853.

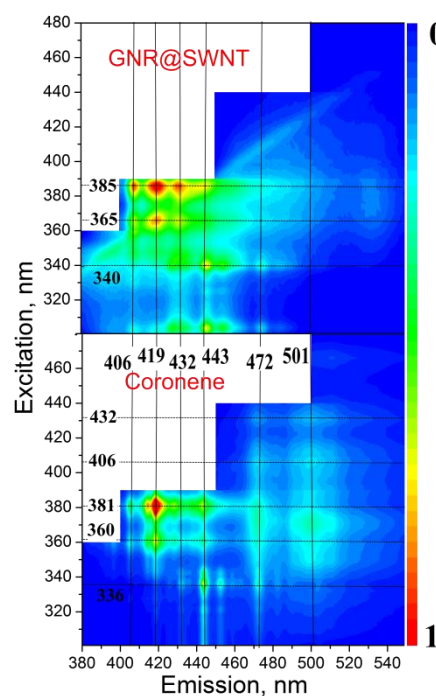


Fig. 1. Photoluminescence excitation map of GNR@SWNT composites and Coronene molecule in a visible range.

**RAMAN DIAGNOSTICS OF ONION-LIKE CARBON**

A.V. Pershina<sup>1,2</sup>, S.N. Bokova<sup>2</sup>, E.D. Obraztsova<sup>2</sup>, K.V. Elumeeva<sup>3,4,5</sup>, A. V. Ishchenko<sup>3</sup>,  
S.I.Moseenkov<sup>3</sup>, V. L. Kuznetsov<sup>3,5,6</sup>

<sup>1</sup> *National Research Nuclear University «MEPhI», Kashirskoe shosse,31, Moscow,Russia*

<sup>2</sup> *A.M. Prokhorov General Physics Institute RAS, 38 Vavilov str., 119991, Moscow, Russia*

<sup>3</sup> *Boreskov Institute of Catalysis SB RAS, Lavrentieva ave. 5, Novosibirsk, 630090, Russia*

<sup>4</sup> *Nikolaev Institute of Inorganic Chemistry, SB RAS, Lavrentieva ave. 3, Novosibirsk, 630090, Russia*

<sup>5</sup> *Novosibirsk State University, Pirogova ave. 2, Novosibirsk, 630090, Russia*

<sup>6</sup> *Novosibirsk State Technical University, K. Marx ave. 20, 630092, Novosibirsk, Russia*

For over forty years, the scientific community has been fascinated by the properties and possible applications of nanodiamond powder produced by detonation of carbon-based explosives. Raman spectroscopy is the most effective method for the diagnosis of carbon systems at the atomic level.

In this work a possibility of the Raman spectroscopy for diagnostics of multi-walled carbon nanotubes and onion-like carbon has been analyzed. Each series consisted of the original material and the material subjected to heat treatment at different temperatures. The Raman spectra were registered using a “Jobin-Yvon S-3000” micro-spectrometer. Samples were excited with the laser line with a wavelength of  $\lambda = 457,9$  nm and  $\lambda = 514,5$  nm at low laser power to avoid heating. In the Raman spectra we revealed the changes corresponding to the structure and characteristics modifications of materials. The basic attention has been paid to D (disorder-induced), G (graphite) and 2D (two-phonon scattering)-bands in the Raman spectra. We investigated several series of nanodiamond powders. Each series consisted of the original material and the material subjected to heat treatment at different temperatures. The spectrum of the initial nanodiamond shows two peaks with a frequency position near 1326 cm<sup>-1</sup> (one thousand three hundred twenty-six) (D-mode) and about 1600 cm<sup>-1</sup> (G-mode). Depending on the increase annealing temperature the D-mode in high frequency area, and the G-mode in the low frequency has been a shifted. In addition, after annealing at a temperature of 1800K or more, there were the appearance of 2D-mode. These changes are explain as the change of state from diamond to graphite (the transition state of sp<sup>3</sup> to sp<sup>2</sup> phase) via the formation of onion-like carbon.

However, studies of other series of nanodiamond powders obtained by different methods shows similar shift dynamics D- and G-modes, but at the same time, it was noted that the phase transition temperature may vary and differ from 1800K.

*This research was partially supported by the RAS research programs and RFBR 12-02-90706-mob\_st.*

## OPTICAL SPECTROSCOPY OF POLYMER SYSTEMS CONTAINING SINGLE-WALL CARBON NANOTUBES

S.N. Bokova<sup>1</sup>, E.D. Obraztsova<sup>1</sup>, T.S. Mamonova<sup>2</sup>, M.V. Shablygin<sup>2</sup> and Y.I. Yuzyuk<sup>3</sup>

<sup>1</sup>A.M. Prokhorov General Physics Institute, RAS, 38 Vavilov street, 119991, Moscow, Russia, [sofia@kapella.gpi.ru](mailto:sofia@kapella.gpi.ru)

<sup>2</sup>A.N. Kosygin Moscow State Textile University, 1 Malaja Kaluzskaja street, 119071, Moscow, Russia

<sup>3</sup>Southern Federal University, 105/42 Bolshaya Sadovaya Str., Rostov-on-Don, 344006, Russia

The aramid fibres serve as a matrix for carbon nanotubes for a wide variety of applications where the reduction of weight, the increase in strength and resistance to corrosion lead to significant improvements in safety and efficiency.

The purpose of this work is to reach a strengthening of aramid fibres by embedding the single-wall carbon nanotubes. A principal potential of SWNTs for introduction in the modern polymeric materials (for instance, for formation of antiballistic fabrics) is based on outstanding mechanical properties of nanotubes: a high degree of elasticity, a feather-weights and a high volume energy absorption.

SWNTs synthesized by arc method (with an average diameter of 1.39 nm) have been used. The preparation technique for SWNT suspensions involves several steps of sonication and ultracentrifugation. The combination of optical methods (Raman scattering and optical absorption) provided a comprehensive characterization of SWNT suspensions. Such suspensions were introduced into the polymer fiber. The introduction was made at the different stages of the process: on a monomer step, on the polymerization step, on the glass fiber step and in course of pulling the soft fiber through the suspension of nanotubes. After the latter treatment, the polymerization process was completed and the test samples were prepared. The mechanical properties of these samples were measured by a set of standard engineering techniques. The strength of fibers with SWNT embedded has been improved up to 10%.

*This research was partially supported by the RAS research programs and RFBR 12-02-90706-mob\_st.*



**Fig.1.** Samples of fibers prepared at different conditions of introduction of nanotubes.

## Synthesis and characterization of $\text{Bi}_2\text{Se}_3$ and $\text{Bi}_2\text{Te}_3$ crystals and flakes

*E.A. Obraztsova<sup>1,2</sup>, N.A. Polgun<sup>1</sup>, A.S. Orekhov<sup>3</sup>, P.V. Shapkin<sup>4</sup>, E.D. Obraztsova<sup>1</sup>*

*1- A.M. Prokhorov General Physics Institute, RAS*

*2 – M.M. Shemyakin & Yu.A. Ovchinnikov Institute of Bioorganic Chemistry, RAS*

*3 – A.V. Shubnikov Institute of Crystallography, RAS*

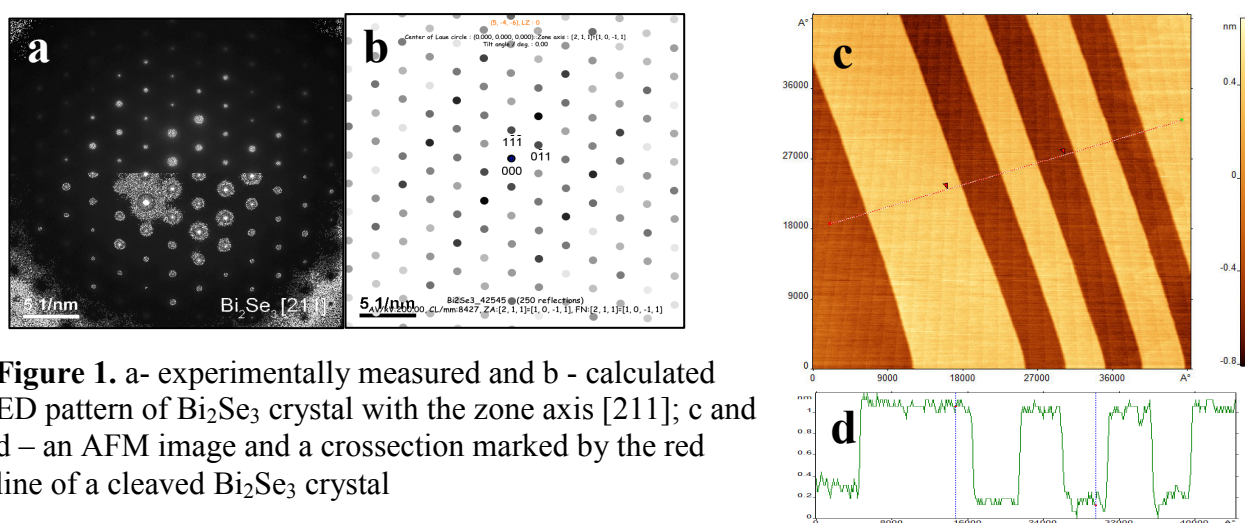
*4 – P.N. Lebedev Physical Institute, RAS*

Two-dimensional structures formed from layered crystals have attracted a great interest due to modification of their properties with decreasing the number of crystalline layers. Most of attention has been paid to graphene – a single layer of carbon atoms arranged in a honeycomb lattice. However it has been predicted theoretically and demonstrated experimentally that many other materials such as boron nitride, gallium selenide and many others exhibit specific properties dictated by a crystalline thickness decreased to a small number of atomic layers.

Lately a detailed study of two-dimensional systems produced from so-called “topological insulators” has started. A topological insulator is a material behaving as an insulator in its interior or bulk shape while permitting the movement of charges on its surface (demonstrating a metallic behavior). Thin layers of these materials (such as  $\text{Bi}_2\text{Te}_3$ ,  $\text{Bi}_2\text{Se}_3$ ) are predicted to be narrow (down to zero) bandgap semiconductors and possess other properties similar to those of graphene such as a linear electron dispersion curves. This makes such nanostructures interesting for both fundamental investigations and technological applications.

In this work we present our results on synthesis and characterization of macroscopic  $\text{Bi}_2\text{Se}_3$  and  $\text{Bi}_2\text{Te}_3$  crystals and the first attempts of a thin layer exfoliation. Samples of monocrystalline  $\text{Bi}_2\text{Se}_3$  and  $\text{Bi}_2\text{Te}_3$  have been synthesized using solvothermal method. The crystals were characterized using atomic force microscopy (AFM), standard and high resolution scanning electron microscopy (SEM), electron diffraction (E) and X-ray energy dispersion spectroscopy. According to these data the monocrystalline  $\text{Bi}_2\text{Se}_3$  phase ( $a=4.14$  nm,  $c=28.63$  nm) has been formed in our experiments. The ED results and the theoretically calculated diffraction pattern of  $\text{Bi}_2\text{Se}_3$  crystal with the zone axis  $[211]$  are presented in Fig 1 (a, b). AFM data demonstrate an easy cleaving for the crystals synthesized provided a smooth surface with a few atomic steps. In Fig. 1 (c,d) a typical image and a cross-section of the surface area of  $\text{Bi}_2\text{Te}_3$  crystal is shown. Thus, we have confirmed that chemical composition and crystalline structure of the crystals synthesized correspond to the desired one. These crystals are good candidates for exfoliation of isolated thin layers due to a small number and a low height of crystalline steps.

As a result of our first attempts to exfoliate such structures from a macroscopic crystal we have already obtained the comparatively thin (10-20 nm) layers. However, according to theoretical calculations, even thinner layers should be obtained for observation of size-induced effects. Further efforts are currently put into fabrication of such structures.



This work was supported by the projects *RFBR- 12-02-31637\_mol\_a*, *12-02-31444-mol\_a*, and by the *Contract 16.513.11.3149 of the Ministry Education and Science of Russian Federation*.

## Ferromagnetic decoration of encapsulated single-walled carbon nanotubes

A.I. Chernov <sup>1</sup>, E.D. Obraztsova <sup>1</sup>, H. Kuzmany <sup>2</sup>

<sup>1</sup> A.M. Prokhorov General Physics Institute, Vavilov str.38, Moscow, Russia

<sup>2</sup> Fakultät für Physik, Universität Wien, Strudlhofgasse 4, 1090 Wien, Austria  
al-chernov@mail.ru

Possibility of application of carbon nanomaterials in spintronics has been actively studied during last years. Recent progress in separation techniques allowed us to investigate the magnetic properties of fully metall-semiconductor separated single-walled carbon nanotubes (SWCNTs).

Spin resonance, magnetic measurements and structural analysis are reported for metal-semiconductor separated SWCNTs after filling with ferrocene. Raman scattering performed after a heat treatment confirms partial transformation to double-walled CNTs but results from spin resonance (FMR), x-ray diffraction and TEM evidence in addition the growth of ferromagnetic nanoparticles. For the metallic tubes the particles are identified as magnetite ( $\text{Fe}_3\text{O}_4$ ) with full chemical stoichiometry. From the temperature dependence of the FMR response (Fig. 1) and from measurements of the magnetization by dc and ac SQUID the magnetite crystals are shown to undergo a Verwey transition. The transition temperature from the SQUID experiment is around 125 K as expected but considerably higher than observed from the FMR analysis. Results for semiconducting tubes are similar but magnetic particles are an order of magnitude smaller and exhibit different structures in addition to magnetite. In addition in this work new nanosystems formed by SWCNT encapsulation - graphene nanoribbons (GNR) inside SWCNTs have been studied with optical methods (Raman spectroscopy, optical spectroscopy, photoluminescence).

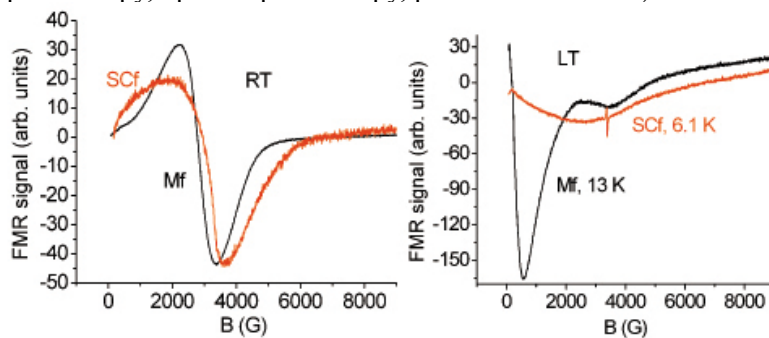


Fig. 1. Ferromagnetic resonance (FMR) for semiconducting and metallic SWCNTs after filling with ferrocene and recorded at 300K (left) and at low temperatures as indicated (right). Response for both nanotube systems are scaled to show approximately the same signal height.

*The work was supported by RAS research programs, RFBR grants 12-02-31581 and 12-02-90805.*

## ALL-OPTICAL INJECTION AND CONTROL OF PHOTOCURRENTS IN UNBIASED GRAPHENE

Petr A. Obraztsov<sup>1,2</sup>, Tommi Kaplas<sup>2</sup>, Sergey V. Garnov<sup>1</sup>, Yuri P. Svirko<sup>2</sup>

<sup>1</sup>*A.M. Prokhorov General Physics Institute, Moscow, Russia*

<sup>2</sup>*Department of Physics and Mathematics, University of Eastern Finland, Joensuu, Finland*

<sup>3</sup>*Physics Department, M.V. Lomonosov Moscow State University, Moscow, Russia*  
p.obraztsov@gmail.com

Owing to a gapless linear band structure and high mobility of massless charge carriers, graphene is considered as a material of future all-wavelength optoelectronics. Recent advances in graphene synthesis and, especially, in the CVD provide production of high quality samples suitable for manufacturing optical and optoelectronic devices. Number of approaches has been proposed to utilize optically/THz excited carriers, whose ultrafast dynamics is still under debate, for electronics. However, most of these approaches require modification of the graphene electronic structure by biasing the sample or introducing a built-in potential at the metal-graphene or graphene-graphene contacts [1]. Another approach suggests injection and coherent control of ballistic photocurrents using third-order nonlinear processes such as quantum interference of one- and two-photon absorption pathways and frequency mixing [2].

We present an alternative all-optical technique to inject the ultrafast currents in unbiased graphene. The proposed method is solely based on a second-order nonlinear effects and therefore provides substantially higher efficiency than latter. In the

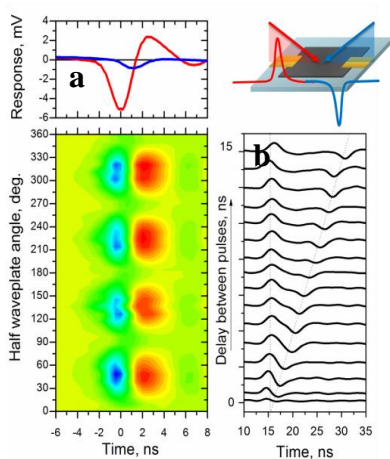


Fig. 1 a) Waveforms and polarization dependence; b) two-beams control of the injected currents.

experiment, we make use of extremely efficient photon-drag effect in graphene, which manifests itself as transfer of the photon momentum to hot electrons during the one-photon interband absorption in graphene [3,4]. The irradiation with intensive linearly polarized femtosecond as well as nanosecond laser pulses in VIS-IR spectral range induces transient picosecond currents in the graphene. The direction and amplitude of the injected currents are completely driven by the orientation of the polarization plane azimuth, angle of incidence and intensity of the pump beam. Moreover, we experimentally demonstrate the possibility of all-optical control of the injected currents by introduction another laser pulse, which incidents at mirror-reflection direction of the first one (Fig.1). In this experimental configuration, the currents injected into graphene are

fully driven by the ratio between the pump pulse intensities and the mutual orientation of their polarizations. The obtained results give new insight on the hot carrier dynamics in graphene, while the opportunity of all-optical control of the transient currents may be implemented in novel optoelectronic and THz devices.

This work was supported by the Russian Foundation for Basic Research (grant 12-02-01369) and Academy of Finland (grant 258220).

[1] T. Mueller, F. Xia, P. Avouris, *Nature Photon.* 4, 297, 2010. [2] D. Sun, C. Divin, J. Rioux, et al., *Nano Lett.* 10(4), 1293, 2010. [3] P.A. Obraztsov, G.M. Mikheev, S.V. Garnov, et al., *Appl. Phys. Lett.* 98, 091903, 2011; [4] J. Karch, P. Olbrich, M. Schmalzbauer, et al., *arXiv:1002.1047v1* (2010).

## STM/STS study of steps at the surface of ternary compound $\text{Bi}_2\text{Te}_2\text{Se}$ .

A.A. Kapustin, V.S. Stolyarov and S.I. Bozhko  
Institute of Solid State Physics RAS, Chernogolovka

STM images and  $dI/dV$  characteristics were measured at the surface of ternary compound  $\text{Bi}_2\text{Te}_2\text{Se}$  both on flat areas and near the steps. We saw steps of two kinds: approximately 1nm height and 0.5nm height. Typical characteristics measured at flat areas and near 1nm steps are demonstrated in Figs.1a,b. They contain a dip (a sharp decrease in the density of states) with a sloping bottom. Near 0.5nm steps, additional peak in the middle of the dip exists (Fig. 2). We do not know the origin of this peak at present. We hypothesize that 0.5nm steps are linear defects which produce new states in the bulk band gap of  $\text{Bi}_2\text{Te}_2\text{Se}$  in addition to the linearly dispersing surface states.

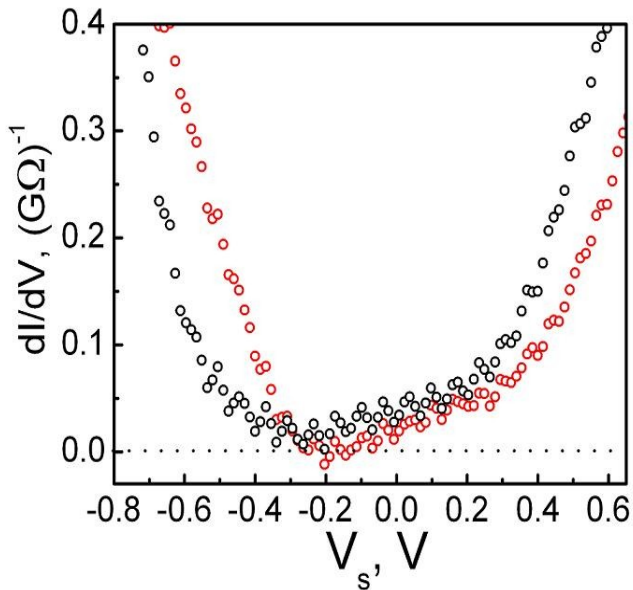


Fig. 1a

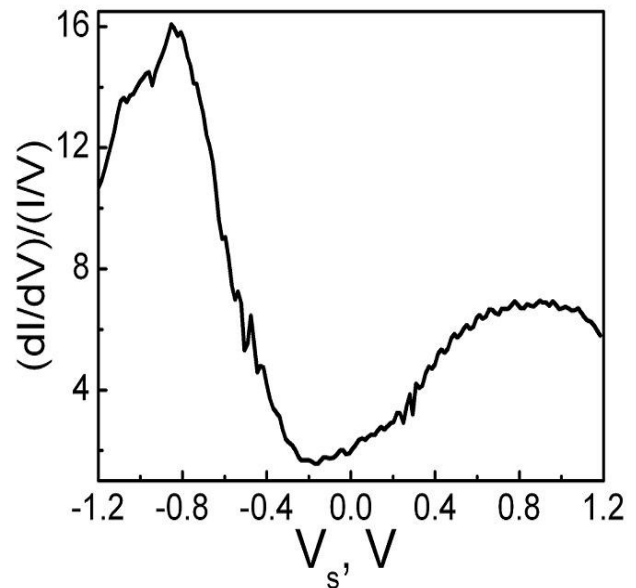


Fig. 1b

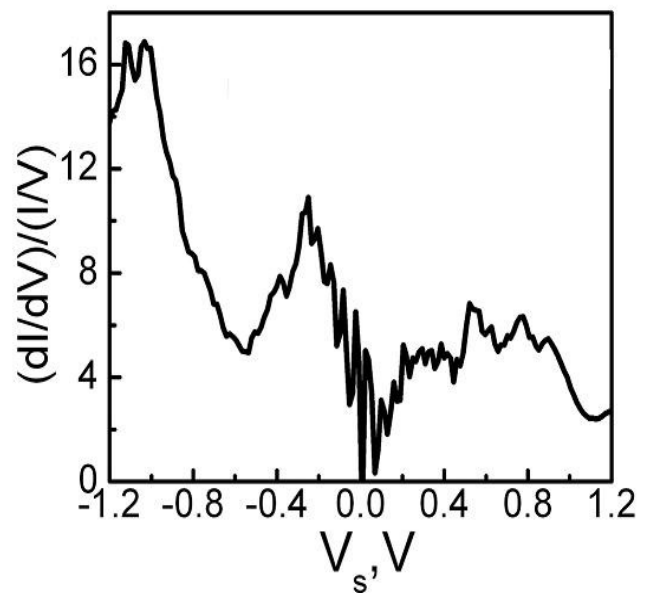


Fig. 2

## **XPS characterization of the surface of coarse-grained and nanostructured titanium and nitinol.**

D.M. Korotin<sup>1</sup>, S. Bartkowski<sup>2</sup>, E.Z. Kurmaev<sup>1</sup>, M. Neumann<sup>2</sup>,  
D.V. Gunderov<sup>3</sup>, R.Z. Valiev<sup>3</sup>.

<sup>1</sup>*Institute of Metal Physics, Russian Academy of Sciences-Ural Division, 620990 Yekaterinburg, Russia*

<sup>2</sup>*Faculty of Physics, University of Osnabruck, 49069 Osnabruck, Germany*

<sup>3</sup>*Institute of Physics of Advanced Materials, Ufa State Aviation Technical University,  
12 K. Marx str., Ufa 450000, Russia*

The results of XPS measurements of coarse-grained (cg) and nanostructured (ns) titanium and nitinol (NiTi) before and after chemical treatment are presented. The ns-Ti and nsNiTi were prepared with help of severe plastic deformation (SPD) [1], and has better mechanical properties than cg-Ti and cg-NiTi. Both cg-Ti and cg-NiTi and both ns-Ti and ns-NiTi were treated in hydrofluoric acid (40% HF, 1 min). It is found that the surface of untreated samples of cg- and ns- titanium and nitinol is covered by amorphous TiO<sub>2</sub> layer. This layer provides the biocompatibility of NiTi and Ti as well prevents the interaction of toxic Ni-constituent from NiTi with environment. According to our measurements the chemical treatment of the samples in hydrofluoric acid reduces the thickness of protective TiO<sub>2</sub> layer and induces the release of Ni from NiTi on the surface enhancing the toxicity of chemically treated nitinol. Finally we have found that the chemical treatment induces an appearance of As on the surface of nitinol and titanium, due to As-contamination in HF [2].

### References:

1. R.Z. Valiev, *Nature Mater.* 3 (2004) 511.
2. I. Fernández-Olmo, J.L. Fernández, A. Irabien, *Separation and Purification Technology* 56 (2007) 118–125.

## Structure of adsorbed fibrinogen studied by single-molecule atomic force microscopy and molecular dynamics simulation

*Protopopova A.D., Tolstova A.P., Zavyalova E.G., Kopylov A.M., Tverdislov V.A., Yaminsky I.V.*

*Lomonosov Moscow State University, Physics Department, Chair of polymer and crystal physics Leninskie gory 1-2, Moscow, Russia, 119991, protopopova@polly.phys.msu.ru*

Atomic force microscopy (AFM) is one of the most promising single-molecule techniques, but it has significant disadvantages. Both the horizontal and vertical dimensions of macromolecules are misrepresented in AFM data. Typically, the vertical dimensions are lower than in reality, and the horizontal dimensions are wider. We propose to use AFM in combination with molecular dynamics (MD) to obtain the detailed data about protein adsorption on single molecule level.

It is widely accepted that one of the initial events that significantly influences biocompatibility of medical biomaterials is the adsorption of proteins from biological fluids onto their surfaces. There are hundreds of proteins in human blood. The total protein concentration is normally 60–80 g/L, and of that number 30–50 g accounts for serum albumin. All of the remaining proteins have significantly lower concentration. The second on the prevalence among blood proteins is immunoglobulin and the third one is fibrinogen. The normal concentration of fibrinogen in blood is 2–4 g/l or 5–9 mM.

A very important thing is that fibrinogen is a key protein in blood clotting and thrombosis. Fibrinogen adsorption onto implant surface turns biomaterials into thrombogenic surfaces. Since people do understand that fibrinogen adsorption plays on the overall biocompatibility, there are many investigations of fibrinogen adsorption onto different surfaces.

The structure of fibrinogen adsorbed on two different surfaces, mica and hexamethyldisilazane-modified mica (HMDS-mica), was investigated using AFM. Data on the height and length of fibrinogen molecules on these substrates agree well with previously published data. The average D-domain height is  $2.2 \pm 0.4$  nm on mica and  $1.2 \pm 0.4$  nm on HMDS-mica. The average length of single fibrinogen molecules is  $42 \pm 7$  nm on mica and  $60 \pm 9$  nm on HMDS-mica. The modeling data agree well with experimental results. Based on the results of AFM experiments, it was initially assumed that the height difference between fibrinogen D-domains on hydrophobic and on hydrophilic surfaces depends mostly on their hydrophobicity. The molecular dynamics simulation results obtained with fibrinogen adsorbing on the two surfaces satisfy this assumption and raise many new questions about the influence of adsorption onto the functional groups of fibrinogen.

## Influence of irregular growth of monoatomic steps during Si/Si(001) epitaxy on generation of surface defects

L.V.Arapkina, V. A. Chapnin, K. V. Chizh, L. A. Krylova, V. A. Yuryev

A. M. Prokhorov General Physics Institute, Russian Academy of Sciences, Moscow, Russia

This report covers investigation of the structural properties of surfaces of Si epitaxial layers deposited on different Si(001) vicinal substrates. Structural properties of the surface epitaxial layers, especially their defects, could affect the growth of nanostructures. We have studied structural properties of the Si epitaxial layers deposited by molecular beam epitaxy (MBE). Experiments were carried out in UHV using GPI-300 high resolution STM coupled with Riber EVA 32 MBE chamber. We have investigated the Si/Si(001) epitaxial layers deposited on the Si(001) wafers tilted  $\sim 0.2^\circ$  to the [110] or [100] direction. We used the standard methods of surface cleaning before MBE. Growth of the epitaxial layers was performed at the temperatures from 360 to 700°C and at different rates of Si deposition. A study of the growth temperature effect on the surface morphology has shown that the step-flow growth is observed at the temperature above 600°C. The structure of the surface depends on its tilt direction and a rate of Si deposition. On the fig.1 STM data for surface Si/Si(001) tilted forward [001] direction are presented. The surface is composed from bent monoatomic steps. In this case every monoatomic step consists of the short parts  $S_A$  and  $S_B$  steps and runs along [001] direction. There are local disarrangements of the structure. We suppose this kind of defects to be connected with a process of transition from the mixed  $S_A + S_B$  monoatomic step to two single  $S_A$  and  $S_B$  steps instead of formation of the  $D_B$  step. For samples tilted to [100] decrease of the Si deposition rate results in appearance of the structure formed by the monatomic steps running along the [110] direction and formation of shapeless pits on the surface instead of the structure formed by the bent monatomic steps running along the [100] direction (fig.2). Change of the tilt direction from [100] to [110] results in appearance of the structure formed by  $S_A$  and  $S_B$  monatomic steps and faceted pits with the rectangle base. On the fig.3 initial stage of the defect formation is shown. There is local stopping of growth  $S_B$  step and appearance of two  $S_A$  steps in this place. In other words we have observed a gap of the  $S_B$  step. These  $S_A$  steps repulse each other and that defect could not be overgrown quickly. The bottom of the deep pit has rectangle shape and a long side of it formed by  $S_A$  step.

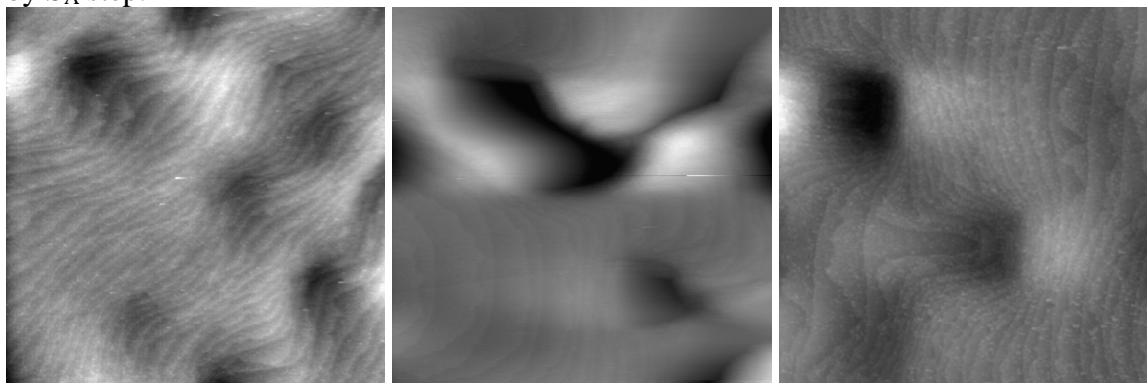


Fig.1 STM image of the surface of the 50nm Si epi-layer deposited at 650°C on Si(001) vicinal wafers tilted  $\sim 0.2^\circ$  towards [001], deposition rate  $\sim 0.3 \text{ \AA}/\text{c}$ .

Fig.2 STM image of the surface of the 50nm Si epi-layer deposited at 650°C on Si(001) vicinal wafers tilted  $\sim 0.2^\circ$  towards [001], deposition rate  $\sim 0.1 \text{ \AA}/\text{c}$ .

Fig.3 STM image of the surface of the 50nm Si epi-layer deposited at 650°C on Si(001) vicinal wafers tilted  $\sim 0.2^\circ$  towards [110], deposition rate  $\sim 0.3 \text{ \AA}/\text{c}$ .



## Index of Authors

- Adamchuk V.K., 4  
Andryushechkin B.V., 1  
Arapkina L.V., 25  
Babichev A.V., 6, 15  
Bakhtizin R.Z., 10  
Bartkowski S., 23  
Bokova-Sirosh S.N., 17, 18  
Borygina K.I., 8  
Bozhko S.I., 22  
Brunkov P.N., 13  
Butko V.Y., 6, 15  
Chapnin V.A., 25  
Chernov A.I., 16, 20  
Chizh K.V., 25  
Dmitriev A., 12  
Egorov A.Yu., 6  
Eltsov K.N., 1  
Elumeeva K.V., 17  
Fahriev V.E., 10  
Fedorov A., 4  
Fedotov N., 12  
Fedotov P.V., 16  
Garnov S.V., 21  
Gasumyants V.E., 15  
Golyashov V.A., 5  
Gunderov D.V., 23  
Gutkin A.A., 13  
Ishchenko A.V., 17  
Kapas T., 21  
Kapustin A.A., 22  
Kierren B., 1  
Kokh K.A., 5  
Kopylov A.M., 24  
Korotin D.M., 23  
Krylova L.A., 25  
Kryzhanovskaya N.V., 6  
Kurmaev E.Z., 23  
Kuzmany H., 20  
Kuznetsov V.L., 17  
Makarenko S.V., 5  
Mamonova T.S., 18  
Marchenko D., 3, 9  
Moseenkov S.I., 17  
Nasibulin A.G., 16  
Nasretdinova V., 12  
Neumann M., 23  
Nikitina E.V., 6  
Obraztsov P.A., 21  
Obraztsova E.A., 19  
Obraztsova E.D., 16–20  
Odobescu A.B., 2  
Orekhov P.V., 19  
Pershina A.V., 17  
Polgun N.A., 19  
Popova A.A., 9  
Protopopova A.D., 24  
Rader O., 3, 9  
Rybkin A.G., 3, 9  
Senkovskiy B.V., 11  
Sevriuk V., 13  
Shablygin M.V., 18  
Shalnev I.V., 13  
Shapkin P.V., 19  
Shikin A.M., 3, 9  
Sobolev M.S., 6, 14  
Stolyarov V.S., 22  
Svirko Y.P., 21  
Talyzin A.V., 16  
Tereshchenko O.E., 5  
Tolstova A.P., 24  
Tverdislov V.A., 24  
Ulyanov P.G., 7  
Usachov D., 4  
Valiev R.Z., 23  
Varykhalov A., 3, 9  
Vilkov O., 4  
Vyalikh D.V., 4  
Yaminsky I.V., 24  
Yuryev V.A., 25  
Yuzuk Y.I., 18  
Zaitsev-Zotov S.V., 2, 12  
Zavyalova E.G., 24  
ZheltoV V.V., 1  
Zhidomirov G.M., 1